DOI: 10.1002/cphc.201701125



Shortfall of B3LYP in Reproducing NMR J_{CH} Couplings in Some Isomeric Epoxy Structures with Strong Stereoelectronic Effects: A Benchmark Study on DFT Functionals

Jasper Adamson, [a] Ryszard B. Nazarski, *[b] Jüri Jarvet, [a, d] Tõnis Pehk, [a] and Riina Aav[c]

Unprecedented scatter plots of calculated versus measured NMR $^{2,3}J_{\text{CH}}$ coupling constants in six densely oxygen functionalized epoxides are found with some B3LYP protocols, an effect attributed to stereoelectronic effects. Hence, 26 other exchange-correlation density functionals (xc DFs) are benchmarked in this work. Very good results are achieved with mPW1PW91 and PBE0 in conjunction with the pcJ-1 basis set (BS) of moderate size. A thorough statistical analysis of 53 relationships between the predicted and observed $^{2,3}J_{\text{CH}}$ datasets is

presented. The effects of some xc DFs, including their x and c parts, and BSs on the calculation results are discussed, also in the context of DFT modeling of electron-density distributions. Moreover, related $^1J_{\text{CH}}$ datasets predicted with 11 different DF methods are considered and compared with the experimental data. Finally, some proposals for further improvement of existing DFs based on the available $^nJ_{\text{CH}}$ (n=1-3) values are briefly outlined, in line with recent results on the DFT electron densities.

1. Introduction

Among the few experimental parameters accessible from solution NMR spectra of (bio)organic compounds, the isotropic indirect nuclear spin–spin coupling constants J_{XV} accompanied by relative chemical shifts δ_X , are valuable sources of structural information on such systems. Vicinal (over three bonds) 1H – 1H and ^{13}C – 1H couplings $^3J_{HH}$ and $^3J_{CH}$ are particularly relevant for the evaluation of spatial relations in configurational and/or conformational analysis. The $^3J_{HH}$ values have found widespread use for determining dihedral angles between the interacting protons. Furthermore, the more scarcely considered heteronuclear $^3J_{CH}$ values can nowadays be routinely determined together with geminal (two-bond) $^2J_{CH}$ data in specifical-

ly dedicated NMR experiments.^[2,3] The $^3J_{\text{CH}}$ data are particularly crucial for all proton-poor systems because of the well-known Karplus-type dependence on geometry.^[4] One-bond and longrange $^{13}\text{C}-^{1}\text{H}$ couplings $^{1}J_{\text{CH}}$ and $^{n}J_{\text{CH}}$ ($n \ge 4$) have also found wide application in modern molecular-structure elucidations.^[5]

The abundance of the aforementioned J_{XY} couplings arising from broad experimental NMR studies is, however, not in an agreement with the capability of current electronic-structure calculations to reliably predict the values of these observables for a wide range of organic entities. Indeed, J values are among the most difficult spectroscopic molecular properties to reproduce quantitatively, especially for large systems. [5a,6] The Kohn-Sham (KS) version of DFT is the preferred tool in this case, owing to its relatively fair treatment of electron-correlation effects at an affordable computational cost. However, KS-DFT accounts for the exchange (x) and correlation (c) energies through a universal exchange-correlation functional of the exact electron density $E_{xc}[\rho(\mathbf{r})]$, for which the true form is unknown. Hence, enormous efforts have been made over the years to find successful approximations for $E_{xc}[\rho(\mathbf{r})]$, known as xc density functionals (xc DFs or simply DFs), which should yield accurate descriptions of structural, energetic, and response properties of the systems of interest.^[7] As a result, there is a large diversity of DFT methods, that is, DF/basis set (BS) combinations, which can be used for predicting the J_{CH} considered here. Nevertheless, to assess the accuracy of numerous DFs in use, benchmarking against accurate experimental data is necessary.

According to the nonrelativistic Ramsey theory of NMR coupling mechanisms, which is sufficient for molecules with firstrow NMR nuclei, the Fermi contact (FC) term is a leading con-

- [a] Dr. J. Adamson, Dr. J. Jarvet, Dr. T. Pehk National Institute of Chemical Physics and Biophysics Akadeemia tee 23, 12618 Tallinn (Estonia)
- [b] Prof. R. B. Nazarski Theoretical and Structural Chemistry Group Department of Physical Chemistry Faculty of Chemistry, University of Lodz Pomorska 163/165, 90-236 Łódź (Poland) E-mail: nazarski@uni.lodz.pl
- [c] Prof. R. Aav Department of Chemistry and Biotechnology Tallinn University of Technology Akadeemia tee 15, 12618 Tallinn (Estonia)
- [d] Dr. J. Jarvet Current address: Department of Biochemistry and Biophysics Arrhenius Laboratories, Stockholm University Svante Arrhenius väa 16, 10691 Stockholm (Sweden)
- Supporting Information and the ORCID identification number(s) for the author(s) of this article can be found under: https://doi.org/10.1002/cphc.201701125.

tribution for a vast majority of isotropic J values.[8] The three other terms are diamagnetic spin-orbit (DSO), paramagnetic spin-orbit (PSO), and spin-dipole (SD) components. The FC term is characterized by electron density near the nuclear positions and thus imposes very rigorous requirements on the quality of the Gaussian-type BSs in the core regions of interacting nuclei. [6,9] Hence, some specifically constructed BSs [10] with tight large-exponent s functions are usually applied for prediction of J values. Although the hybrid B3LYP^[11] approximation is most often used, [9a,c,10e,11e,12] several other DFs [6,9b,11f,12c,f,g,k,l,n,r,13] are also employed. Except for one recent paper,[13e] however, these DFs were not optimized for the calculation of J_{XY} values, as opposed to such attempts concerning NMR chemical shieldings $\sigma_{\rm X}$.[11f,13e,14] Furthermore, neither of these two spectroscopic parameters were considered in typical benchmarking studies of DFs for their use in chemistry and physics. [15]

The above-outlined landscape of the state-of-the-art firstprinciples prediction of J couplings in medium-sized molecules is indeed to some extent ambiguous. Some of deficiencies and perspectives in this field were recently presented. [12k,l,n] Among them, computations of J for systems with triple bonds^[12k] or lone-pair-bearing electronegative atoms^[5a, 6, 12d,l,r] have been widely explored. However, there is a lack of complete studies on the performance of all commonly available J-calculation-oriented BSs used with different promising DFs. Moreover, a large part of the earlier KS-DFT works concerns relatively small and simple molecules. Hence, more general conclusions were drawn with difficulty from such data. For instance, several calculations of J_{CH} in carbohydrates and their derivatives were reported, $^{[12a,b,e]}$ but, to the best of our knowledge, only one critical paper dealing with the use of a few DFs for the prediction of ¹J_{CH} in other saturated electron-rich and conformationally rigid compounds was published.[12g]

Herein, we supplement the above-mentioned lack of benchmarking analyses by reporting a study on $J_{\rm CH}$ in six isomeric (15,55)-3-alkoxy-6,7-epoxy-2-oxabicyclo[3.3.0]octanes $1-6^{[16]}$ (Figure 1). These J values were measured in CDCl₃ solution at 800 MHz 1 H NMR spectrometer frequency and calculated by means of a variety of DF methods. Stereorelations between the three constituent rings were previously established by analysis of experimental $^{3}J_{\rm HH}$ values, supported by their DFT-B3LYP prediction. Diastereomeric epoxides 1-6 afforded 225 unique J couplings (67 $^{1}J_{\rm CH}$, 70 $^{2}J_{\rm CH}$, and 88 $^{3}J_{\rm CH}$). All these J values were considered as components of the two attached $J_{\rm CH}$ datasets (see Supporting Information): 2,3JCH_EPOXY ($-7 < J^{\rm obsd} < 9$ Hz) and 1JCH_EPOXY ($126 < J^{\rm obsd} < 185$ Hz). The analysis of such relatively large databases of $J_{\rm CH}$ values collected exclusively in one NMR laboratory is noteworthy in itself. On the

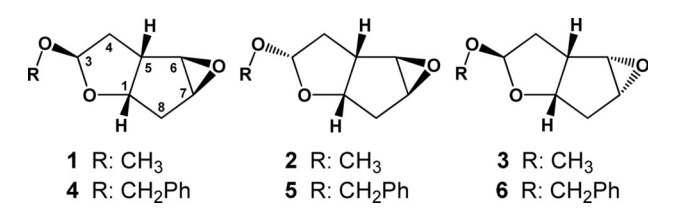


Figure 1. The six epoxy compounds 1–6 of this study.

contrary, discrepancies in J_{CH} values are observed frequently in measurements from different laboratories. [12], 17]

The following points were addressed in this work: 1) initial probing of a set of magnetic-property-oriented double/triple- ζ BSs used in conjunction with B3LYP as a reference DF against experimental $^{2,3}J_{CH}$ values in epoxides **1–6**, 2) identification of some unexpectedly revealed subsets of $^{2,3}J_{CH}$, 3) further testing the other DFT methods, that is, combinations of some more accurate DFs with the "best" BS (pcJ-1) recognized in step 1, 4) additional examination of selected promising DF approaches in calculating the $^{1}J_{CH}$ data, and 5) statistical error analysis of all important results obtained in steps 1–5.

To the best of our knowledge, this kind of a widespread study focusing on DFT-based prediction of $^nJ_{\text{CH}}$ in computationally demanding electron-rich molecules has not yet been published. In fact, this work is the first benchmarking study of KS-DFT calculations of $^{2,3}J_{\text{CH}}$ values. The CPU times for the usage of all available Gaussian-type NMR/EPR-specialized BSs were also not determined previously. Moreover, our conclusions and proposals can aid the construction of better DFs in the future.

Computational Details

Geometry Optimizations

All molecular structures of flexible systems 1-6 were computed starting from their MMX (1986)^[18] geometries created with PCMO-DEL.[19] Specifically, an extensive conformational search for preferred forms was carried out with an internal GMMX randomize subroutine of the above program, in a similar manner to that described elsewhere. [120] Further cascade geometry refinement of low-energy candidate conformers was done with the Gaussian 09 package. [20] The Hartree-Fock/DFT hybrid Becke three-parameter Lee-Yang-Parr xc functional (B3LYP)[11] was finally used with the 6-311 + G(d,p) BS in restricted KS-DFT calculations. Equilibrium structures optimized at this level of theory were also used in a critical test of some computational methods for prediction of $\delta_{\rm H}$ and $\delta_{\rm C}$ values.[21] The "Tight" SCF and Opt convergence criteria were applied to ascertain accuracy. [12m,o,22] A fine-pruned (150,590)[23] numerical integration grid was used, owing to soft modes arising from the dynamic phenomena of methyl-group rotations. [20] Analogous optimizations were performed with the hybrid PBEO DF (also known under the acronym PBE1PBE).[24]

To simulate the impact of the CDCl₃ solvent on the structures and NMR spectroscopic behavior of the studied solutes, an equilibrium solvation protocol^[25] of an integral equation formalism/polarizable continuum model (IEF-PCM)^[26] scheme was used. The Gaussian 09 default parameters (including the UFF^[27] atomic radii) were applied when constructing solute cavities, whereby a cavity is understood as a free space inside a bulk solvent. A few calculations were also performed with nonstandard IDSCRF atomic radii,[28] which were found beneficial in recently reported structure optimizations^[120] and calculations of NMR chemical shifts. $^{\!\scriptscriptstyle [29]}$ The UA0 model and unscaled ($\alpha = 1$) van der Waals surfaces were used in this case, and related input files were produced with the SCRF-RADII program. [30] The Cartesian coordinates of all ten finally considered conformational structures of epoxides 1-6 are listed in Table S9 (Supporting Information), and their Chemcraft^[31] molecular representations are shown in Figure S2.

Moreover, harmonic vibrational frequencies $\omega_{\rm e}$ were evaluated analytically in the framework of the DFT method used for geometry optimization to verify whether all located stationary points represented true local/global minima ($N_{\rm imag} = 0$) on the molecular Born-Oppenheimer potential-energy hypersurfaces of all systems and to determine their Gibbs free energies G° at standard ambient temperature and pressure (298.15 K, 1 atm), that is, at the NMR recording temperature of 298 K. In turn, for assessing relative abundances of individual forms of much more mobile epoxides 4-6 in conformational equilibria, the energy-weighted Boltzmann population (molar fraction p) of each entity was calculated by applying the Boltzmann distribution function $p_i = e^{-\Delta G_i^o/R} / \sum_j e^{-\Delta G_j^o/RT}$, where j is the number of structures in thermal equilibrium, R the ideal gas constant, T the system temperature (set to 298.15 K), and ΔG° ; the ΔG value of the *i*th form relative to the energy of the most stable form. In such calculations of p_i for multiconformer systems, [11f] relative total energies $\Delta E_{{\rm tot},i}$ are sometimes used as approximated weighting factors instead of ΔG_i data.^[32]

Calculation of J_{CH} Values

In our initial prediction of ¹³C-¹H J values, B3LYP was used in conjunction with the nine BSs developed specifically to provide accurate values of NMR^[10a,c-f] or EPR^[10b] parameters. The IEF-PCM(UFF,CHCl₃)/B3LYP/6-311 + G(d,p) optimized geometries of the ten low-energy forms of systems 1-6 were employed; for all details, see Supporting Information. The following BSs of valence double/triple-ζ polarized (or better) quality were examined: IGLO-II,^[10a] IGLO-III,^[10a] EPR-III,^[10b] aug-cc-pVTZ-J,^[10c] ccJ-pVTZ,^[10d] pcJ-1,^[10e] aug-pcJ-1, $^{[10e]}$ pcJ-2, $^{[10e]}$ and 6-311 + + G^{**} -J. $^{[10f]}$ An EPR-III dataset was used as is stored internally in Gaussian 09, while the others were downloaded from the EMSL Basis Set Library.[33] Moreover, the decontracted Pople-type 6-311 + G(d,p) BS was generated with the "NMR = mixed" keyword and used only for calculating the dominant FC terms. [9c] In this particular case, all of the three remaining contributions to ${\it J}$ (i.e. SD, PSO, and DSO terms) were found with the unmodified contracted 6-311+G(d,p) set. Though rovibrational effects [9b,12c,k,22a,34] can be non-negligible in ${}^{n}J_{CH}$ values, especially for n=1, they were generally not considered here, since their evaluation is extremely demanding computationally for large molecules; a similar approach was taken by other authors. [12f]

In the second step, a set of 26 other selected DFs (some historical as well as more recent ones) accessible within Gaussian 09^[20] were used in conjunction with pcJ-1, which was initially found to be the best BS from the viewpoint of novelty, result reliability, and very short CPU time. Thus, the performance of subsequent DFs (given in chronological order) was examined: BLYP, [11a,b,d] BP86, [11b,35] PW91, [36] BPW91, [11b,36] B3PW91, [11b,c,36b] B3P86, [11b,c,35] PBE, [37] B1LYP, [38] PBE0,^[24] mPW1PW91,^[36b,39] OP86,^[35,40] OLYP,^[11a,d,40] OPW91,^[36b,40] $\mathsf{OPBE},^{[37,40]} \quad \mathsf{O3LYP},^{[11a,d,40a,41]} \quad \mathsf{B97-2},^{[42]} \quad \mathsf{CAM-B3LYP},^{[43]} \quad \mathsf{LC-}\omega \mathsf{PBE},^{[44]}$ BMK, $^{[45]}$ HSE06 (sometimes also called HSE), $^{[46]}$ M06-L, $^{[47]}$ M06-2X, $^{[48]}$ ω B97X,^[49] ω B97X-D,^[50] APF,^[51] and APF-D.^[51] These single-point jobs were carried out with Gaussian 09. [20] The IEF-PCM(radii,CHCl₃) approach was used in both steps of NMR calculations. The J values computed for each of the three mutually exchanging H atoms in the methyl groups were arithmetically averaged to produce a single J_{CH} value for each methyl group as a whole. The same also concerns the J data for the ortho and meta positions of the phenyl ring. The five so-called pure d functions were employed for all non-H atoms. The CPU execution times of prediction of all J values in molecule 4 were also measured for the DFT methods tested here; for all details, see the Supporting Information.

The computed versus experimental J_{CH} correlations were analyzed by a linear regression model, and predicted J_{CH} values were plotted against the observed values in the usual way. [112h,i,m,22c] The greater value of the Pearson correlation coefficient r or its square r^2 was considered as a very simple indication of better adjustment of the compared J data (vide infra). In addition, the four standard statistical metrics for errors, namely, the root-mean-square deviation (RMSD), [12c] mean absolute deviation (MAD= $(1/n)\Sigma_i|J_i^{\text{calcd}}-J_i^{\text{obsd}}|$, where n is the total number of J_{CH} values), [12,53] corrected RMSD, [12c] that is, $CRMSD = [(1/n)\Sigma_i|J_i^{\text{corr}}-J_i^{\text{obsd}}|$, were used as much more reliable estimates of the uncertainties of calculation results. Moreover, maximum positive or negative deviations between the J_i^{calcd} (or J_i^{corr}) and J_i^{obsd} data, that is, $\max(+/-)$, [13d,50] were evaluated. All statistical analysis was performed with the Excel spreadsheet.

2. Results and Discussion

2.1. Structures

First, we performed a conformational analysis of all of the flexible tricyclic systems 1-6.[16] The present benchmarking study secures the reliability of results with an exhaustive conformational search. Three forms A-C of 1-3 and four forms A-D of **4–6** were found within the energy window of $\Delta E_{\rm tot}$ 16.4 kJ mol⁻¹ (see Computational Details and Supporting Information). The ΔE_{tot} and ΔG° values obtained in KS-DFT calculations and Boltzmann weightings of all individual contributing forms, that is, percentage relative populations $P = 100 p_{ii}$ estimated from such different energetic data are presented in Table S3. A scrutiny of $P_{E,i}$ and $P_{G,i}$ values revealed that only equilibrium geometries of rotamers A of 1-3 and the six lowenergy rotamers of type A and B of 4-6 can be considered in practice (for details, see Supporting Information); molecular drawings of all considered conformations of 1-6 are shown in Figure S2.

2.2. Assessment of J-Oriented Basis Sets

Ten specialized BSs were tested in conjunction with the widely used B3LYP. A linear least-squares model was applied with scaling and shifting factors, [12k] that is, the slope a and intercept b, respectively. So, regression equations of type (1) were considered:

$$J_{\text{CH}}^{\text{calcd}} = aJ_{\text{CH}}^{\text{obsd}} + b$$
 (1)

Two kinds of J couplings, namely, $^2J_{\rm CH}$ and $^3J_{\rm CH}$, measured for systems 1–6, forming a compact series of $J_{\rm CH}^{\rm obsd}$ ranging from -7 to 9 Hz (see the 2,3JCH EPOXY database in the Supporting Information), were analyzed initially. Their negative values for a normal set of $^2J_{\rm CH}$ data (vide infra) were determined by means of calculations. The strongest correlation between the observed and unscaled raw $^{2,3}J_{\rm CH}$ data was found with IGLO-II (for the related plot, see Figure S3), while the weakest one was found with IGLO-III (Figure S4). The resulting $r_{\rm all}^2$ (n=2, 3) data are listed in Table 1 and Tables S4 and S5, together with the values of other metrics. A vast majority of the used specialized BSs afforded comparable results; their performance is present-

Table 1. Correlations and statistics for 12 selected B3LYP/BS calculations of ^{2,3} J _{CH} values in systems 1–6. [a,b]											
Basis set	r^2 (n = 2, 3)	Intercept a [Hz]	Slope <i>b</i>	RMSD [Hz]	CRMSD [Hz]	MAD [Hz]	CMAD [Hz]	mp6	$r_{\mathrm{O-2a}}^{2}$ [c]	CPU time ^[d]	GPs/CPU time ratio ^[e]
IGLO-II	0.9925	0.4028	0.9480	0.51	0.37	0.41	0.30	0.9104	0.9311	1.00 ^[f]	2.55
aug-pcJ-1	0.9892	0.5637	0.9833	0.69	0.44	0.58	0.37	0.9183	0.9383	9.96	0.42
pcJ-1	0.9883	0.5725	0.9876	0.72	0.46	0.61	0.38	0.9326	0.9533	1.06	3.02 ^[g]
EPR-III	0.9862	0.6173	0.9654	0.75	0.50	0.61	0.42	0.8713	0.8916	8.95	0.53
6-311 + G** Mixed	0.9860	0.5989	0.9700	0.74	0.51	0.61	0.42	0.8424	0.8621	1.93	1.74
6-311 + + G**-J	0.9859	0.6240	0.9973	0.80	0.51	0.67	0.42	0.8296	0.8500	2.97	1.22
pcJ-2	0.9858	0.6640	0.9865	0.81	0.51	0.68	0.42	0.8745	0.8955	9.72	0.69
ccJ-pVTZ	0.9853	0.6636	0.9876	0.82	0.52	0.69	0.43	0.9067	0.9278	7.10	0.81
aug-cc-pVTZ-J	0.9852	0.6858	0.9983	0.86	0.52	0.72	0.43	0.8604	0.8952	30.64	0.22
IGLO-III	0.9825	0.7097	0.9030	0.84	0.57	0.62	0.47	0.8627	0.8855	4.15	0.91
IGLO-II/ IDSCRF	0.9923	0.4078	0.9479	0.52	0.37	0.42	0.31	0.9173	0.9383	1.00	2.55
pcJ-1/ IDSCRF	0.9880	0.5769	0.9874	0.72	0.47	0.61	0.39	0.9391	0.9598	1.07	3.02 ^[g]

[a] The 2,3JCH_EPOXYdatabase was used. [b] Boldface indicates the best values in each column, and the worst ones are underlined. [c] The r^2 values for the five remaining $^{2,3}J_{CH}$ subsets are listed in Table S4. [d] Relative to the time required for B3LYP/IGLO-II calculations of all J values in **4.** [e] Gaussian primitives (GPs)/CPU time ratio. [f] Execution time: 250 min; for the used computational resources, see Supporting Information. [g] The ratio of 804 GPs/266 min.

ed graphically in Figure 2. All these B3LYP-based methods have a tendency to overbind, that is, positive deviations $(J^{calcd}-J^{obsd})$ are larger than negative, in line with other similar literature data that are not fully satisfactory from the theoretical point of view, that is, with approximately 10–14% overestimation. [34d] However, any scaling [34d] of raw $^{2,3}J_{CH}$ for compounds **1–6** would not serve its purpose, because of their roughly parallel arrangement (Figure 3).

Nevertheless, it is highlighted that the best performance of B3LYP combined with IGLO-II mentioned above can only be attributed to a fortunate cancellation of errors in this DFT method (see Supporting Information for more details). IGLO-II was followed by aug-pcJ-1 and pcJ-1. A benefit of using aug-pcJ-1 over pcJ-1 is most likely derived from the presence of additional diffuse functions in aug-pcJ-1. Such functions are crucial in handling molecules with lone-pair electrons on heteroatoms. [12a,b,d,g,54] Regarding the other B3LYP-based methods, we note that the so-called mixed basis set procedure of Deng et al. [9c] applied here afforded practically the same results as

the much more time-consuming use of EPR-III. For further discussion on the remaining BSs, concerning the CPU time measurements, see the Supporting Information.

Quite unexpectedly, remarkably scattered data points were found in the plots of B3LYP-calculated versus observed $^{2,3}J_{CH}$ data. A close examination of Figure 3 and Figures S3-S5 permitted the three types of J-coupling subsets to be separated into normal, oxygenic a (O-a), and oxygenic b (O-b) in both $^2J_{CH}$ and ${}^{3}J_{CH}$ datasets (Table 2). Undoubtedly, the reason for these surprising plots arises from numerous carbon-oxygen bonds of different polarity in the studied systems 1-6. They contain a dioxygenated (acetal) carbon atom and a highly strained three-membered oxirane ring, which both are most likely responsible for specific stereoelectronic effects for the O-2b subset. In turn, spin-spin interactions are transmitted via etheric oxygen atoms in all the O-3 cases. (Table 2; see also Supporting Information). Also, different orientations of O-C-H hydrogen atoms to vicinal lone electron pairs can provoke dramatic changes in ${}^{1}J_{CH}$ involving the \underline{H} nuclei (cf. the Perlin Effect), [55]

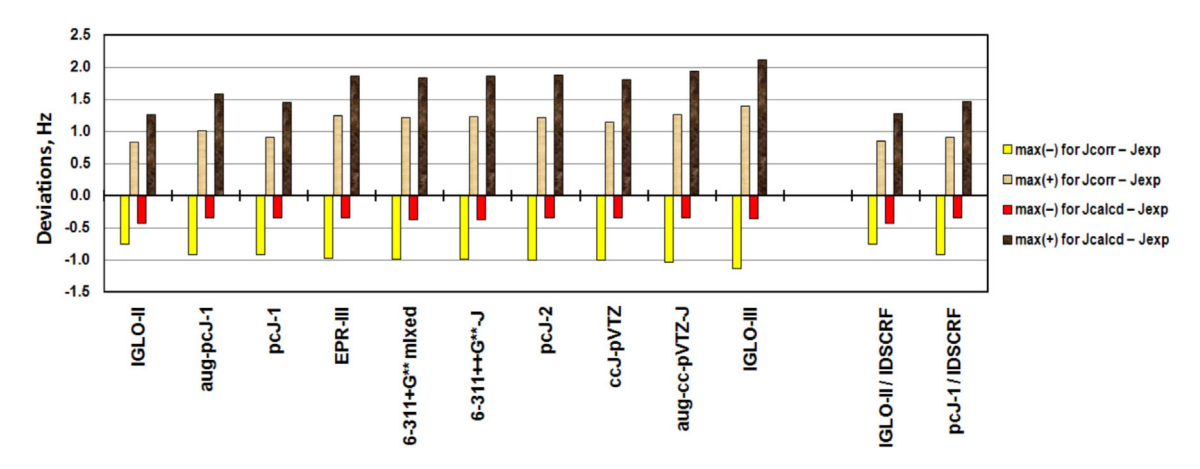


Figure 2. The performance of 12 applied B3LYP/BS methods in terms of the max(+/-) deviations in $^{2,3}J_{CH}$ values in systems 1–6. For all numerical data, see Table S4.

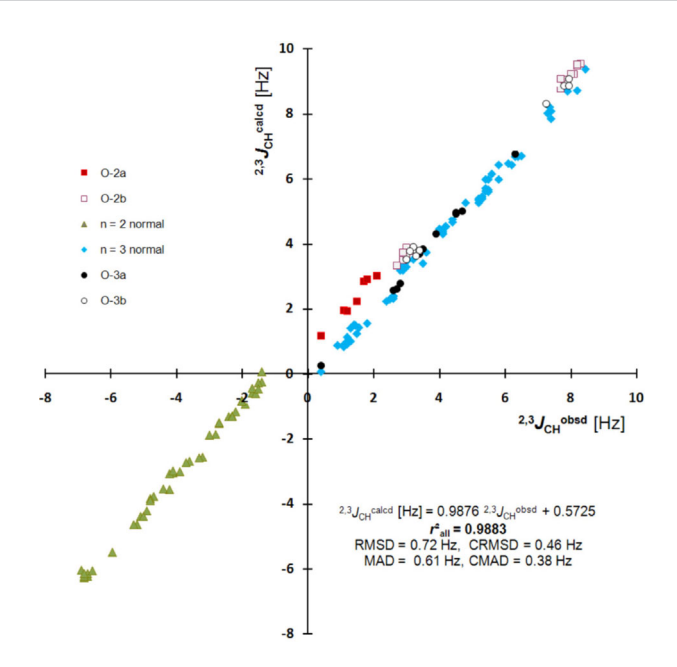


Figure 3. The scatter relationship between 158 B3LYP/pcJ-1 calculated and experimental $^{2.3}J_{\rm CH}$ values in systems **1–6.** For all numerical data, see Table S1.

	• •	l-containing fragmen n the underlined nuc	
n=2 O-2a	O-2b	n=3 O-3a	O-3b
О- <u>С</u> -С- <u>Н</u> О-С-С- <u>Н</u>	OTHF - C - C - H O Oepoxy - C - C - H		<u>></u> C-O-C-∏

which usually are explained as resulting from the redistribution of electron density in the C– \underline{H} bond produced by hyperconjugative^[56] or dipolar^[13b] interactions. One can suppose that similar effects also concern related ${}^2J_{\text{CH}}$ and ${}^3J_{\text{CH}}$ values.

Such an unprecedentedly large differentiation of J couplings mentioned above afforded five or six regression equations of type (1) related to 5–6 straight lines, which were found for each of the used DFT methods; for pertinent statistics, see Table 1 and Tables S4 and S5. Two additional metrics, namely, mp6 data (i.e., multiplication products found by multiplication of all six distinct r^2 data concerning the six subsets of $^{2.3}J_{\rm CH}$) and $r^2_{\rm O-2a}$ related to the O-2a units are also given in Table 1. The $r^2_{\rm O-2a}$ data were found to be very variable and most influence the mp6 values. Intriguingly, the use of IDSCRF^[28] instead of UFF^[27] radii in the IEF-PCM scheme afforded slightly larger magnitudes of these two metrics at the expense of $r^2_{\rm all}$ ($n\!=\!2$, 3); see Table 1.

An impact of (di)oxygenated carbon atoms involved in $^2J_{\rm CH}$ and $^3J_{\rm CH}$ couplings in some acyclic compounds (early literature

data) was considered in the so-called *J*-based approach. [57] In the context of this work, most important are more recent calculation results on the molecular fragments $\underline{\mathsf{C}}-\mathsf{O}-\mathsf{C}-\underline{\mathsf{H}}$ and $\underline{\mathsf{C}}-\mathsf{C}-\mathsf{C}(-\mathsf{O})-\underline{\mathsf{H}}.^{[12e,58]}$ In turn, the $^2J_{\mathsf{CH}}$ values in a few heteroaromatic systems were subjected to a natural bond orbital (NBO) analysis. [12]] The NBO approach to $^nJ_{\mathsf{CH}}$ values was also recently applied with the DU8c method, [17] in which empirical scaling of the dominant FC terms in the formulated three multiterm predictive equations was performed by multivariate regression analysis. As a result, the three types of $^nJ_{\mathsf{CH}}$ values (n=1-3) were examined separately. [17]

Therefore, we concluded that our findings are excellent examples of an "undesirably high specialization" in the B3LYP prediction of J_{CH} . Undoubtedly, various stereoelectronic effects are operative in molecules **1–6**, which strongly modify related J values in the spirit of the Karplus-like relations mentioned above. Indeed, plots with such scattered points of the calculated versus observed $^{2,3}J_{\text{CH}}$ data are reported for the first time, to the best of our knowledge. However, at a reliable DFT level, all such effects should be adequately reflected by one equation of type (1) and not by 5–6 relationships, and the B3LYP approximation does not properly account for the interactions of this kind. Hence, it was necessary to seek better computational protocols. For this reason, we resorted to various other DFT approaches involving more accurate DFs to overcome the problem.

2.3. Assessment of Other KS-DFT Functionals

To understand and explain the results described above, 26 other DFs, found in a post-local spin-density approximation way^[7] and belonging to different rungs of the Jacob's ladder^[59] of KS-DFT functionals, were additionally applied for prediction of $^{2,3}J_{CH}$ in systems **1–6**. Thus, 27 DF approaches including 1) generalized-gradient approximations (GGAs) BP86, BLYP, PW91, BPW91, PBE, OP86, OLYP, OPW91, and OPBE, 2) globalhybrid GGAs (GH-GGAs) B3PW91, B3LYP, B3P86, B1LYP, O3LYP, B97-2, PBE0, mPW1PW91, APF, and APF-D, 3) meta-GGAs BMK and M06-L, 4) GH meta-GGA functional M06-2X, and 5) rangeseparated hybrid (RSH) GGAs CAM-B3LYP, LC-ωPBE, ωB97X, ωB97X-D, and HSE06 were all used here (for appropriate references, see Computational Details; for the DF families, see ref. [15b]). The key results obtained in conjunction with the pcJ-1 BS are listed in Table 3 together with measured CPU times. The performance of all tested DFs is also presented graphically in Figure 5. As above with B3LYP, positive deviations ($J^{calcd}-J^{obsd}$) are usually much larger than negative deviations. The three exceptions are LC-ωPBE, BMK, and especially

Scrutiny of all these results revealed that the most accurate DF in prediction of $^{2.3}J_{\text{CH}}$ values is mPW1PW91, followed very closely by PBE0 ($r_{\text{all}}^2 = 0.9975$ and 0.9973, respectively); for the mPW1PW91/pcJ-1 data, see Figure 4. Related magnitudes of the slope a/intercept b are also good (1.023/0.028 and 1.020/0.072, respectively). Thus, all three regression parameters are close to their ideal values of 1, 1, and 0, respectively, while large magnitudes of $r_{\text{O}-2a}^2$ are also found. Simultaneously, re-

DF	r^2 (n = 2, 3)	Slope a	Intercept <i>b</i> [Hz]	RMSD [Hz]	CRMSD [Hz]	MAD [Hz]	CMAD [Hz]	mp6	r_{O-2a}^{2} [c]	CPU time ^{[d}
mPW1PW91	0.9975	1.0226	0.0284	0.25	0.21	0.20	0.17	0.9449	0.9728	1.49
PBE0	0.9973	1.0196	0.0721	0.26	0.22	0.21	0.17	0.9491	0.9761	1.46
HSE06	0.9971	1.0058	0.1026	0.26	0.23	0.21	0.18	0.9405	0.9666	1.36
LC-ωPBE	0.9970	0.9683	-0.0954	0.31	0.23	0.25	0.19	0.9242	0.9595	1.62
APF or APF-D	0.9966	1.0020	0.1421	0.29	0.25	0.24	0.20	0.9418	0.9676	1.49
M06-2X	0.9959	1.0382	0.2385	0.45	0.27	0.37	0.21	0.8992	0.9292	<u>3.62</u>
BMK	0.9952	1.2194	-0.2134	1.02	0.30	0.84	0.24	0.9074	0.9644	3.45
ωB97X-D	0.9951	0.9315	0.2490	0.42	0.30	0.32	0.24	0.9039	0.9282	1.58
ωB97X	0.9950	0.9234	0.2505	0.44	0.30	0.35	0.24	0.9355	0.9635	1.63
B3PW91	0.9949	0.9771	0.2403	0.37	0.30	0.31	0.25	0.9259	0.9503	1.44
B1LYP	0.9942	1.0452	0.3758	0.61	0.33	0.51	0.27	0.9544	0.9767	1.48
CAM-B3LYP	0.9934	0.9862	0.3981	0.51	0.35	0.43	0.28	0.9256	0.9485	1.51
B97-2	0.9926	0.9472	0.3620	0.49	0.37	0.39	0.30	0.9524	0.9742	1.46
B3P86	0.9919	0.9529	0.3787	0.51	0.38	0.42	0.32	0.9158	0.9394	1.44
O3LYP	0.9908	0.9864	0.3379	0.51	0.41	0.42	0.34	0.9509	0.9769	_[e]
B3LYP	0.9883	0.9876	0.5725	0.72	0.46	0.61	0.38	0.9326	0.9533	1.44
OPW91	0.9874	0.9404	0.2660	0.54	0.48	0.47	0.41	0.9226	0.9635	1.04
OPBE	0.9873	0.9389	0.2683	0.54	0.48	0.47	0.41	0.9200	0.9613	1.04
OP86	0.9811	0.9145	0.4314	0.70	0.59	0.60	0.51	0.9162	0.9556	1.04
M06-L	0.9801	1.3873	<u>-1.4765</u>	<u>1.98</u>	0.61	<u>1.50</u>	0.51	0.6577	0.7532	2.83
OLYP	0.9785	0.9693	0.6050	0.83	0.63	0.67	0.54	0.9371	0.9668	1.03
BPW91	0.9716	0.9208	0.7745	0.97	0.73	0.78	0.62	0.8653	0.8904	1.01
PW91	0.9681	0.9179	0.8473	1.05	0.77	0.84	0.66	0.8600	0.8854	1.01
PBE	0.9680	0.9199	0.8528	1.05	0.77	0.84	0.66	0.8793	0.9054	1.00 ^[f]
BP86	0.9603	0.8941	0.9458	1.16	0.86	0.92	0.74	0.8517	0.8775	1.01
BLYP	0.9530	0.9421	1.1769	1.41	0.94	1.13	<u>0.80</u>	0.8792	0.9052	1.00
mPW1PW91/ IDSCRF	0.9975	1.0224	0.0333	0.25	0.21	0.20	0.17	0.9488	0.9766	1.48
PBE0/ IDSCRF	0.9973	1.0194	0.0770	0.27	0.22	0.21	0.18	0.9526	0.9795	1.46
PBE0 & geometry	0.9950	1.0274	0.0594	0.35	0.30	0.27	0.24	0.8828	0.9354	1.46
APF (APF-D)/ IGLO-II	0.9974	0.9731	-0.0112	0.25	0.22	0.21	0.18	0.9210	0.9472	1.39

[a] The 2,3JCH_EPOXY database was applied. [b] Boldface indicates the best values, and the worst ones are underlined. [c] The r^2 values for the five remaining subsets of r^2 values are listed in Table S4. [d] Relative to the time required for PBE/pcJ-1 calculations of all J_{XY} values in system 4. [e] Not estimated due to a known bug in Gaussian 09, Revision D.01. [f] Execution time: 185 min; for the used computational resources, see Supporting Information.

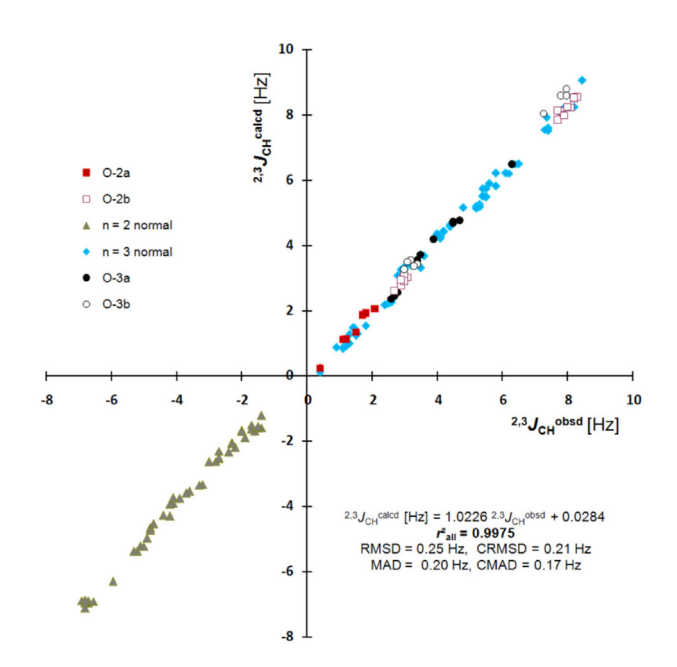


Figure 4. The relationship between 158 mPW1PW91/pcJ-1 calculated and experimental $^{2,3}J_{\rm CH}$ values for systems **1–6.** For all numerical data, see Table S1

gression coefficients of all the six related highly specific equations have become rather similar, especially for PBEO (see Tables S4 and S5).

The intercept b values near to zero found for both top DFs practically fulfill the requirements of a "linear scaling approach" introduced by Bally and Rablen in their comparative study on a variety of DFT methods for computing $^{2-4}J_{\rm HH}$. [60] Statistics of some data for molecules 1–6, rescaled according to this approach with b=0, are listed in Table S7. Note, however, that in this model of the relationship $J_{\rm XY}^{\rm calcd}$ versus $J_{\rm XY}^{\rm odsd}$, [60] all of the rovibrational corrections (vide supra) to the $^nJ_{\rm XY}$ values under analysis should be taken into account. By omitting this condition, approximate predictive Equation (2) can be proposed for the results obtained at the best mPW1PW91/pcJ-1 level of theory (see also related discussion in the Supporting Information)

$$^{2,3}J_{CH}^{scaled} = 0.9755 \times ^{2,3}J_{CH}^{calcd}$$
 (2)

Four further DFs, namely, HSE06, LC- ω PBE, and APF(-D), were found to be a little worse in respect of their $r_{\rm all}^2$ values. However, LC- ω PBE is much degraded by the large max(+/-) deviation (Table S4). The (GH) meta-GGAs, three RSH-GGAs,

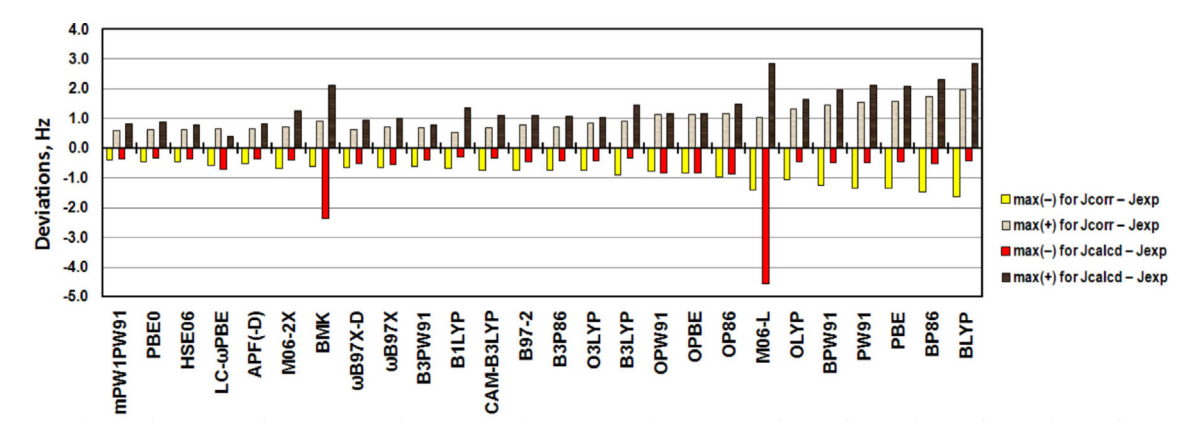


Figure 5. The performance of 27 used DF/pcJ-1 methods in terms of the max(+/-) deviations in $^{2,3}J_{CH}$ values in systems 1–6. For all numerical data, see Table S4

and single-parameter B1LYP GH-GGA DFs all failed. Despite the M06-2X results still fulfilling the two main criteria required for a "well-performing protocol" ($r^2 \ge 0.995$ and $0.95 \le \text{slope } a \le 1.095$ 1.05), [61] related max(+) and mp6 parameters are too large and too small, respectively. Similarly, very large RMSD, MAD, and max(+/-) values were found with BMK, despite the potentially good r_{all}^2 data. In fact, this heavily parameterized DF was designed for thermochemical kinetic studies and not for NMR calculations. Highly unreliable results with BMK were previously reported in prediction of ¹³C NMR chemical shifts.^[21] In turn, a mid-ranked position of M06-L, with the poorest a, b, RMSD, and MAD data, coincides well with the poor performance of this DF in predicting $^{2-4}J_{\rm HH}$. [60] Hence, we concluded that the $r_{\rm all}^2$ value is not a perfect measure of goodness of fit between the J_{XY} under comparison. Indeed, the RMSD and MAD values are much better indicators of this goodness. Finally, the observed irregularity in magnitudes of $r_{\rm O-2a}^2$ and mp6 (Table 3) can be explained by the lack of a systematic hierarchy of DFs leading to highly unsystematic behavior of typical DFT methods.

A cross-comparison of ${}^{2,3}J_{CH}$ found by some of the DF/pcJ-1 approaches was especially interesting to us. An illustrative plot between the mPW1PW91 and B3LYP results (Figure S9) shows two approximately straight lines formed by ${}^2J_{CH}$ and ${}^3J_{CH}$ data points. This important comparison, free from all kinds of measurement errors, indicates that the above two types of J coupling are quite differently reproduced by the two methods. The ${}^{3}J_{CH}$ data points form a roughly linear fit with intercept b close to 0 Hz, while the b value for the ${}^2J_{CH}$ points is about -1 Hz. In other words, the B3LYP-based ²J_{CH} values are uniformly overestimated by about 1 Hz with respect to the experimental and mPW1PW91-predicted values. Thus, B3LYP is only a little better in this regard than the nonhybrid DFs such as BLYP, BP86, and PBE (for details, see the Supporting Information). The semilocal exchange component of mPW1PW91 has improved long-range behavior, [39] while B3LYP does not properly model the electron-density distribution far away (i.e. 3-10 Å) from the nuclei. [62] Therefore, it might be expected that the ²J_{CH} and ³J_{CH} values predicted with B3LYP will be good and poor, respectively. However, the reverse situation is found.

Overall, the three-parameter GGAs perform much better than their parent DFs (Table 3). This generalization in J_{CH} prediction is identical with the conclusion drawn from detailed comparisons of KS-DFT electron densities with those from high-level ab initio correlated calculations. A significant effect of the BS on the DFT-modeled electron densities, which also is strongly dependent on the applied DFs, was shown in ref. [63].

For further results and discussion on all remaining xc DFs, showing a parallelism in computing NMR data ($\sigma_{\rm X}/\delta_{\rm X}$ and $J_{\rm XY}$) and the benefit of using of some functionals over others, as well as concerning the impact of individual x and c components of xc DFs on the calculation outputs, please refer to SI.

2.4. Prediction of ¹J_{CH} Values

In the final stage of this study, selected DF/pcJ-1 methods were used in calculations of one-bond 13 C- 1 H J values in 1–6. These protocols were chosen from among a few of the most promising DF approaches tested above. In addition, the results achieved with some mid- and low-ranked DFs were considered for the purpose of comparison. The relationships between 67 observed and unmodified raw $^{1}J_{\text{CH}}$ values are shown in Figure 6, and pertinent error statistics are provided in Table 4. A few sets of points form some straight lines with different slopes, starting roughly from the origin of the experiment–theory coordinates. The external lines arise from the BLYP and B3LYP (top, b > 0), and LC- ω PBE and APF/IGLO-II (bottom, b small or < 0), respectively. Thus, the $^{1}J_{\text{CH}}$ values predicted with BLYP and B3LYP are overestimated, while those obtained by using LC- ω PBE and APF are underestimated.

Table 4 reveals that the best DF is mPW1PW91, followed by PBE0 and APF. The remaining ${}^{1}J_{\text{CH}}$ datasets arising from the HSE06 and B3LYP/IGLO-II protocols are worse. All other methods are strongly degraded by relatively large RMSDs. Thus, the LC- ω PBE results gave the greatest RMSD of 10.03 Hz, despite an r^2 value of 0.9987. In turn, the BLYP and B3LYP outputs (with pcJ-1) are very similar, whereas the latter are only slightly better. The latter result, confirming similar ${}^{1}J_{\text{CH}}$ findings of Max-

7

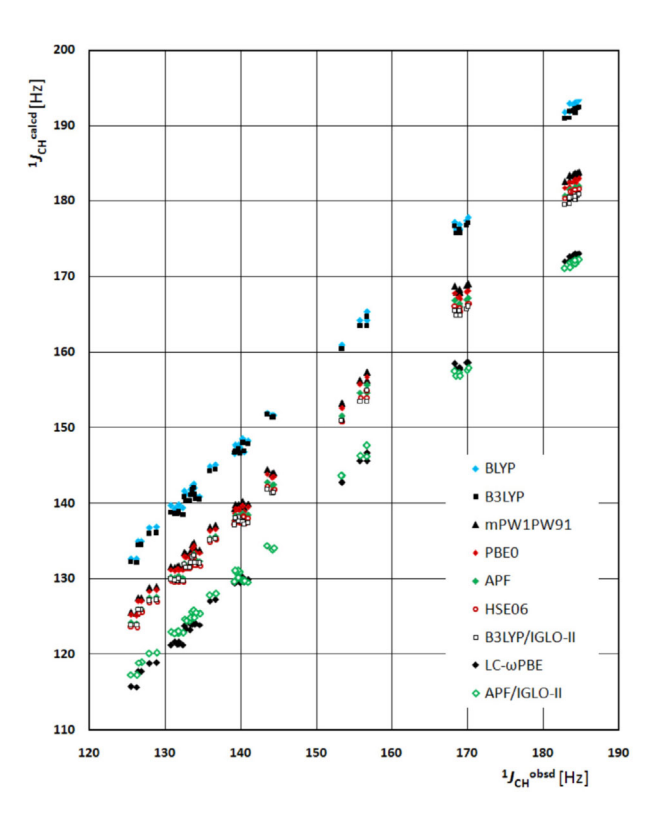


Figure 6. The relationship between the nine sets of DF/pcJ-1 (or IGLO-II) calculated and experimental ${}^{1}J_{CH}$ values for systems **1–6**. The main error metrics are given in Table 4. For all numerical data, see Table S2.

imoff et al.,^[9b] is in sharp disparity to a significant differentiation of the BLYP and B3LYP outputs for $^{2,3}J_{\text{CH}}$ values (Table 3). Our results, which do not support the assertion of the above authors that PW91 and PBE are the most accurate DFs for $^{1}J_{\text{CH}}$ values,^[9b] are in line with the more recent conclusions of Keal et al. on such a performance of PBE,^[12c] all statistics related to additional data for systems **1–6** are given in Table S8. Finally, we note that the use of IGLO-II combined with APF or B3LYP

consistently produces $^1J_{CH}$ values which are smaller by about 8.5 and 10 Hz, respectively, that is, by about 6%, than those found with pcJ-1.

On the whole, the uncertainties in predicted ¹J_{CH} values are greater than those for $^{2,3}\emph{J}_{\text{CH}}$ values but do not exceed 0.4% of the average value of analyzed experimental $^1J_{\text{CH}}$ data (\approx 157 Hz). Comparison between $^{n}J_{CH}$ (n=1-3) determined with BLYP, OLYP, OP86, and OPBE or OPW91 by using pcJ-1 was also interesting for us (Tables S1 and S2). Thus, the choice of Handy's OPTX exchange (O),[40] as a semi-local correction to the local Slater exchange, [11d,20,64] gives $^1J_{CH}$, $^2J_{CH}$, and $^3J_{CH}$ values about 15, 0.85, and 0.25 Hz smaller, respectively, than those predicted with Becke88 exchange (B)[11b] (OLYP vs. BLYP). This result is in full agreement with the conclusion that DFs with B exchange are always outmatched in predicting electron-charge densities by their DF counterparts with O exchange. [65] In turn, the use of the PBE correlation gives $^1J_{\text{CH}}$, $^2J_{\text{CH}}$, and $^3J_{\text{CH}}$ values that are about 13, 0.5, and 0.3 Hz smaller, respectively, than those computed with LYP correlation^[11a,d] (OPBE vs. OLYP). A similar trend was found for replacement of LYP through P86 (OP86 vs. OLYP), in line with related results on the DFT electron densities.^[65] All of these facts explain, at least in part, the discrepancy between ²J_{CH} values predicted with B3LYP and mPW1PW91 (see above and the Supporting Information), because analytical expressions of the semilocal correlation components of PW91 and PBE are very similar.[37] (JCH values found with the two latter DFs also are virtually identical; Table 3 and Tables S5 and S6). Our ${}^{1}J_{CH}$ data are consistent with the approximately 20 Hz difference in ¹J_{PH} values in the PH₃ molecule reported for the correlation functionals LYP and PBE.[13d]

In the light of the foregoing (see also the Supporting Information), it is evident that mutual impacts of tested xc DFs (strictly speaking, their approximate x and c parts) as well as BSs on calculated $^nJ_{\text{CH}}$ values considered here are substantial and very complicated. This result is in full harmony with similar conclusions from the above-mentioned works on the DFT-predicted electron densities. $^{[63,65]}$

		BLYP	B3LYP	mPW1PW91	PBE0	APF	HSE06	B3LYP/IGLO-II	LC-ωPBE	APF/IGLO-I
¹J _{CH}	$r_{\rm all}^2 \ (n=1)$	0.9989	0.9990	0.9990	0.9990	0.9990	0.9988	0.9989	0.9987	0.9985
	slope a	1.0126	1.0092	0.9857	0.9772	0.9759	0.9792	0.9574	0.9723	0.9304
	intercept b [Hz]	6.2173	6.1030	2.1198	2.8010	1.9664	1.0578	4.0102	- <u>6.0123</u>	0.5859
	RMSD [Hz]	7.92	7.30	0.63	0.98	1.81	2.21	2.56	10.03	9.78
	CRMSD [Hz]	0.65	0.58	0.56	0.57	0.57	0.63	0.62	0.62	0.72
	MAD [Hz]	7.71	7.11	0.52	0.77	1.62	2.03	2.29	<u>9.77</u>	9.45
	CMAD [Hz]	0.51	0.46	0.45	0.45	0.46	0.49	0.49	0.49	<u>0.55</u>
^{1–3} ∫ _{CH}	$r_{\rm all}^2 \ (n=1-3)$	0.9998	0.9999	1.0000	1.0000	1.0000	1.0000	0.9999	0.9999	1.0000
	slope a	1.0463	1.0457	0.9990	0.9946	0.9876	0.9852	0.9812	0.9335	0.9338
	intercept b [Hz]	1.0232	0.5056	0.0855	0.1362	0.1807	0.1467	0.3676	-0.0734	0.0640
	RMSD [Hz]	4.59	4.14	0.42	0.58	1.02	1.23	1.48	<u>5.58</u>	5.46
	CRMSD [Hz]	0.93	0.64	0.41	0.44	0.41	0.43	0.54	0.64	0.47
	MAD [Hz]	<u>3.21</u>	2.65	0.30	0.38	0.66	0.77	1.00	3.21	3.09
	CMAD [Hz]	0.85	0.54	0.30	0.32	0.30	0.31	0.43	0.44	0.34

8





2.5. Combining the Present J_{CH} Results

What is the relation between the best methods found in predicting $^{2,3}J_{\text{CH}}$ to those achieved in calculations of $^{1}J_{\text{CH}}$? Should these two J data subsets be considered together or separately? From the analysis of the contents of Tables 3 and 4, it is evident that the best result was always found by the mPW1PW91/pcJ-1 method. The slopes a and intercepts b found for $^{1-3}J_{\text{CH}}$ values are very close to 1 and 0, respectively. However, individual a values of 0.986 and 1.023 found for $^{1}J_{\text{CH}}$ and $^{2,3}J_{\text{CH}}$ are somewhat different. This strongly suggests that certain physically real quantity/ties responsible for J_{CH} values belonging to both these J-coupling subsets is/are captured by an approximate analytical expression of mPW1PW91 in some internuclear-distance-dependent way. The worse DFs involve PBE0, APF, and HSE06.

The above discussion indicates that, in order to obtain good results, the two $J_{\rm CH}$ ranges in question should be considered individually. The same conclusion can be drawn from the inspection of very similar $^1J_{\rm CH}$ values found by using BLYP and B3LYP (with pcJ-1) as opposed their strongly diverse results in $^{2,3}J_{\rm CH}$ values (vide supra). In fact, only by separate analysis of these two $J_{\rm CH}$ subsets was it possible to observe a large differentiation of the results for molecules **1–6**, depending on the KS-DFT method used. Such $J_{\rm CH}$ data subsets were also considered separately in other papers cited above. [12p,17,53] Clearly, all J values within these $J_{\rm CH}$ ranges should be correctly reproduced by the sought universally applicable DFT method.

For further results and discussion on the optimized molecular geometries and the great analogy between the DFT prediction of $\sigma_{\rm X}/\delta_{\rm X}$ and $J_{\rm XY}$ values, see the Supporting Information.

3. Conclusions

We have reported a systematic benchmarking study on a series of KS-DFT methods used for accurate prediction of NMR $^nJ_{\text{CH}}$ ($n\!=\!1\!-\!3$) couplings in a series of six electron-rich epoxides $1\!-\!6$, measured in CDCl $_3$ solution. These tricyclic diastereomers with carbon atoms in different environments containing etheric oxygen atoms were quite unexpectedly found to be challenging systems for routine B3LYP-based computations of $^nJ_{\text{CH}}$ values. Hence, it is the first DFT study dealing with the impact of this type of local chemical environments on $^{13}\text{C}^{-1}\text{H}$ J couplings. Generally, the performance of diverse DF methods in providing a prediction of $^{2,3}J_{\text{CH}}$ values was not reported to date. The CPU times for all currently available BSs developed specifically for calculations of NMR/EPR parameters were also not determined previously. To summarize our main conclusions:

1) The use of B3LYP combined with nine BSs designed for prediction of magnetic properties is insufficient for a correct reproduction of $^{2,3}J_{CH}$ in epoxides 1–6. Indeed, three types of *J*-coupling subsets were thus recognized in both series of $^{2}J_{CH}$ and $^{3}J_{CH}$ values; see the 2,3JCH EPOXY database (Supporting Information). Such an unprecedentedly large differentiation of J_{CH} values in 1–6 was rationalized by ste-

- reoelectronic effects operative in these molecules, which arise from the presence of many fragments that contain C—O bonds of different polarity.
- 2) The success of the best B3LYP/IGLO-II method, reported previously and in part confirmed here, was attributed to a very fortunate cancellation of the intrinsic errors of this method. So, its use in such NMR calculations should be rather abandoned in favor of other, more accurate DFT approaches. The variant of a "mixed basis set" procedure of Deng et al. applied in this work afforded practically the same results as the much more time-consuming use of EPR-III. Hence, the new pcJ-1 BS, with good calculation reliability and very favorable cost-to-benefit ratio, was selected for all further studies.
- To understand the origin of the aforementioned differentiation of ^{2,3}J_{CH} in a wider perspective, 26 other xc DFs were examined in conjunction with pcJ-1. The results were compared in a systematic fashion and contrasted to those achieved by using the mPW1PW91 and PBE0 hybrids, which were recognized as the best performers among all of the tested DFs. Accordingly, the approximate predictive Equation (2), consistent with a linear scaling approach of Bally and Rablen, [60] was proposed. It was also, inter alia, found that experimental ${}^2J_{CH}$ values are overestimated by about 1.5–2 Hz by using nonhybrid DFs, while related ${}^3J_{CH}$ values are reproduced relatively well. In this respect, B3LYP is only a little better than the pure DFs. Thus, the choice of DF was identified as the most critical methodological variable for J_{CH} predictions. More specifically, a moderate percentage (25%) of nonlocal Fock exact exchange in the used DFs turned out to be crucial for good performance in evaluation of J_{CH} . Besides, the parallelism existing between DF predictions of $\sigma_{\rm X}/\delta_{\rm X}$ and $J_{\rm XY}$ values was demonstrated. Mutual effects of a few xc DFs (including their x and c parts) and BSs were also considered, and their great and complex influence on predicted J_{CH} was shown. A very large coincidence between all these conclusions and some literature results on DFT modeling of electron charge density^[63,65] was emphasized.
- 4) The above results were found to be suitable for prediction of $^1J_{CH}$ values in **1–6** (see the 1JCH_EPOXY database in the Supporting Information). In this case, mPW1PW91/pcJ-1 data followed closely by related PBE0 results were recognized to be the most accurate. The mPW1PW91/pcJ-1 method was also found to be the best approach for both series of $^1J_{CH}$ and $^{2,3}J_{CH}$ data to be analyzed separately. Moreover, these two J_{CH} ranges must be considered individually. Obviously, the sought exact (universal) DFT approach should correctly reproduce all J_{CH} couplings as important NMR observables independent of reference and external magnetic field and easily accessible to modern instrumentation. Hence, the two combined ranges of J_{CH} values mentioned above could be used in the search for such an improvement.
- 5) Our best results for J_{CH} values were found with the DFs ranked recently by Medvedev et al.^[66] as yielding the best electron-density distributions (APF-D (2), PBE0 (4) and



mPW1PW91 (12), where the numbers are ranking positions of the 128 considered DFs) or affording small errors in chemically relevant density differences (insights from the Fukui function);^[67] unfortunately, mPW1PW91 was not analyzed in ref.[67]. In turn, M06-L, found here to be inappropriate for J_{CH} predictions, was ranked among the three DFs yielding the worst densities^[66] or larger errors in the Fukui function.^[67] The same is true of BMK,^[66,67] which also gave large RMSDs and MADs in this ^{2,3}J_{CH} study. The conclusions of Medvedev et al. were confirmed recently by Mezei et al.[68] All of these facts, which are in very good agreement with the foregoing discussion, indicate that there is a strong correlation between the accurate reproduction of NMR σ_X/δ_X and especially J_{XY} experimental data and faithful modeling of the exact electron-density distribution in core regions of the nuclei in question by the used DFs. This hypothesis seems to be an important guideline for all further studies on both closely interrelated research areas (KS-DFT development and accurate prediction of NMR parameters).

Briefly, we recommend the mPW1PW91/pcJ-1//B3LYP/6-311 + G(d,p) methodology used within the IEF-PCM(UFF,CHCl₃) scheme for predicting ¹⁻³ $J_{\rm CH}$ values in (bio)organic molecules, particularly those containing numerous diverse C—O bonds or other similarly difficult bonding patterns. At the same time, two new large $J_{\rm CH}$ databases are proposed for easy future testing of various other KS-DFT methods in this regard.

Acknowledgements

The authors acknowledge Silver Sun and Kalle Kaljuste for preliminary NMR measurements. They also thank to Prof. Craig P. Butts (University of Bristol, Bristol, UK) for his remarks to an early online version of this article. R.B.N. thanks to Prof. De-Cai Fang (Beijing Normal University, Beijing, China) for providing the SCRF-RADII program and Dr. Piotr Matczak (University of Lodz) for help in installing this software, measurements of CPU times, and an insightful discussion on the early draft. R.B.N. thanks also to the Rector of the University of Lodz for financial support within the Faculty grant "Basic research". This research was supported by the computing facilities of the ACC Cyfronet (AGH University of Science and Technology, Kraków, Poland) under Grant No. MNiSW/Zeus lokalnie/UŁódzki/016/2013 and in part by PL-Grid Infrastructure (Prometheus supercomputer)—all these grants to R.B.N. The work was further supported by the Estonian Ministry of Education and Research through Grant Nos. PUT692 and IUT23-7 and the EU European Regional Development Fund (Grant Nos. 3.2.0101.08-0017 and TK134).

Conflict of interest

The authors declare no conflict of interest.

Keywords: conformation analysis \cdot density functional calculations \cdot NMR spectroscopy \cdot oxygen heterocycles \cdot spin-spin coupling constants

- [1] a) M. Karplus, J. Chem. Phys. 1959, 30, 11–15; b) "NMR in Organic Structural Elucidation": H. Conroy in Advances in Organic Chemistry. Methods and Results, Vol. 2 (Eds.: R. A. Raphael, B. C. Taylor, H. Wiberg), Interscience Publ. Inc., New York, 1960, pp. 265–328; c) M. Karplus, J. Phys. Chem. 1960, 64, 1793–1798; d) M. Karplus, J. Am. Chem. Soc. 1963, 85, 2870–2871.
- a) N. Nath, Lokesh, N. Suryaprakash, ChemPhysChem 2012, 13, 645-660;
 b) T. Parella, J. F. Espinosa, Prog. Nucl. Magn. Reson. Spectrosc. 2013, 73, 17-55.
- [3] For a brief overview of related NMR techniques, see the Measurement Methodology section in the Supporting Information.
- [4] J. A. Schwarcz, A. S. Perlin, Can. J. Chem. 1972, 50, 3667 3676.
- [5] a) "Spin-Spin Coupling Constants with HF and DFT Methods": T. Helgaker, M. Pecul in Calculation of NMR and EPR Parameters: Theory and Applications (Eds.: M. Kaupp, M. Bühl, V. G. Malkin), Wiley-VCH, Weinheim, 2004, Chapter 7, pp. 101 121; b) E. Kleinpeter, A. Koch, K. Pihlaja, Tetrahedron 2005, 61, 7349 7358; c) R. Araya-Maturana, H. Pessoa-Mahana, B. Weiss-López, Nat. Prod. Commun. 2008, 3, 445 450.
- [6] T. Helgaker, M. Jaszuński, M. Pecul, Prog. Nucl. Magn. Reson. Spectrosc. 2008, 53, 249 – 268.
- [7] a) "Density-Functional Approximations for Exchange and Correlation": V. N. Staroverov in A Matter of Density: Exploring the Electron Density Concept in the Chemical, Biological, and Materials Sciences (Ed.: N. Sukumar), Wiley, Hoboken, 2013, pp. 125–156; b) A. D. Becke, J. Chem. Phys. 2014, 140, 18A301; c) "Density Functional Theory (DFT) and Time Dependent DFT (TDDFT)": V. P. Gupta in Principles and Applications of Quantum Chemistry, Elsevier Inc., London, 2016, Chapter 5, pp. 155– 194
- [8] S. A. Perera, R. J. Bartlett, Adv. Ouantum Chem. 2005, 48, 434 467.
- [9] a) J. E. Peralta, G. E. Scuseria, J. R. Cheeseman, M. J. Frisch, Chem. Phys. Lett. 2003, 375, 452–458; b) S. N. Maximoff, J. E. Peralta, V. Barone, G. E. Scuseria, J. Chem. Theory Comput. 2005, 1, 541–545; c) W. Deng, J. R. Cheeseman, M. J. Frisch, J. Chem. Theory Comput. 2006, 2, 1028–1037.
- [10] a) "The IGLO-Method: Ab Initio Calculation and Interpretation of NMR Chemical Shifts and Magnetic Susceptibilities": W. Kutzelnigg, U. Fleischer, M. Schindler in NMR—Basic Principles and Progress, Vol. 23 (Eds.: P.; Diehl, E. Fluck, H. Günther, R. Kosfeld, J. Seelig), Springer, Berlin, 1991, pp. 165–262; b) V. Barone, J. Chem. Phys. 1994, 101, 6834–6838; c) P. F. Provasi, G. A. Aucar, S. P. A. Sauer, J. Chem. Phys. 2001, 115, 1324–1334; d) U. Benedikt, A. A. Auer, F. Jensen, J. Chem. Phys. 2008, 129, 064111; e) F. Jensen, Theor. Chem. Acc. 2010, 126, 371–382; f) H. Kjær, S. P. A. Sauer, J. Chem. Theory Comput. 2011, 7, 4070–4076.
- [11] a) C. Lee, W. Yang, R. G. Parr, *Phys. Rev. B* 1988, *37*, 785–789; b) A. D. Becke, *Phys. Rev. A* 1988, *38*, 3098–3100; c) A. D. Becke, *J. Chem. Phys.* 1993, *98*, 5648–5652; d) B. G. Johnson, P. M. W. Gill, J. A. Pople, *J. Chem. Phys.* 1993, *98*, 5612–5626; e) J. R. Cheeseman, G. W. Truck, T. A. Keith, M. J. Frisch, *J. Chem. Phys.* 1996, *104*, 5497–5509; f) K. W. Wiitala, T. R. Hoye, C. J. Cramer, *J. Chem. Theory Comput.* 2006, *2*, 1085–1092.
- [12] See, e.g., a) F. Cloran, I. Carmichael, A. S. Serianni, J. Phys. Chem. A 1999, 103, 3783 – 3795; b) R. Stenutz, I. Carmichael, G. Widmalm, A. S. Serianni, J. Org. Chem. 2002, 67, 949-958; c) T. W. Keal, T. Helgaker, P. Sałek, D. J. Tozer, Chem. Phys. Lett. 2006, 425, 163-166; d) O. E. Taurian, R. H. Contreras, D. G. De Kowalewski, J. E. Pérez, C. F. Tormena, J. Chem. Theory Comput. 2007, 3, 1284-1294; e) M. Tafazzoli, M. Ghiasi, Carbohydr. Res. 2007, 342, 2086 – 2096; f) R. Suardíaz, C. Pérez, R. Crespo-Otero, J. M. García de la Vega, J. San Fabián, J. Chem. Theory Comput. 2008, 4, 448-456; g) A. C. Neto, F. P. dos Santos, A. S. Paula, C. F. Tormena, R. Rittner, Chem. Phys. Lett. 2008, 454, 129-132; h) R. B. Nazarski, Phosphorus Sulfur Silicon Relat. Elem. 2009, 184, 1036-1046; i) S. Leśniak, A. Chrostowska, D. Kuc, M. Maciejczyk, S. Khayar, R. B. Nazarski, Ł. Urbaniak, Tetrahedron 2009, 65, 10581-10589; j) R. H. Contreras, F. P. dos Santos, L. C. Ducati, C. F. Tormena, Magn. Reson. Chem. 2010, 48, S151-S158; k) J. San Fabián, J. M. García de la Vega, R. Suardíaz, M. Fernández-Oliva, C. Pérez, R. Crespo-Otero, R. H. Contreras, Magn. Reson. Chem. 2013, 51, 775 – 787; I) J. San Fabián, J. M. García de la Vega, E. San Fabián, J. Chem.

- Theory Comput. **2014**, 10, 4938–4949; m) R. B. Nazarski, W. Makulski, *Phys. Chem. Chem. Phys.* **2014**, 16, 15699–15708; n) A. Navarro-Vázquez, *Magn. Reson. Chem.* **2017**, 55, 29–32; o) R. B. Nazarski, P. Wałejko, S. Witkowski, *Org. Biomol. Chem.* **2016**, 14, 3142–3158; p) T. Helgaker, M. Jaszuński, P. Świder, *J. Org. Chem.* **2016**, 81, 11496–11500; q) A. Gryff-Keller, P. Szczeciński, *RSC Adv.* **2016**, 6, 82783–82792.
- [13] a) O. L. Malkina, D. R. Salahub, V. G. Malkin, J. Chem. Phys. 1996, 105, 8793–8800; b) G. Cuevas, K. Martínez-Mayorga, M. C. Fernández-Alonso, J. Jiménez-Barbero, C. L. Perrin, E. Juaristi, N. López-Mora, Angew. Chem. Int. Ed. 2005, 44, 2360–2364; Angew. Chem. 2005, 117, 2412–2416; c) G. Palermo, R. Riccio, G. Bifulco, J. Org. Chem. 2010, 75, 1982–1991; d) B. Pudasaini, B. G. Janesko, J. Chem. Theory Comput. 2013, 9, 1443–1451; e) M. Alipour, RSC Adv. 2015, 5, 4737–4746.
- [14] T. W. Keal, D. J. Tozer, J. Chem. Phys. 2003, 119, 3015-3024.
- [15] a) K. E. Riley, B. T. Op't Holt, K. M. Merz, Jr., J. Chem. Theory Comput. 2007, 3, 407–433; b) R. Peverati, D. G. Truhlar, Philos. Trans. R. Soc. A 2014, 372, 20120476.
- [16] R. Aav, T. Pehk, S. Tamp, T. Tamm, M. Kudrjašova, O. Parve, M. Lopp, Magn. Reson. Chem. 2011, 49, 76–82.
- [17] A. Kutateladze, O. A. Mukhina, J. Org. Chem. 2015, 80, 10838 10848.
- [18] "MMX: An enhanced version of MM2": J. J. Gajewski, K. E. Gillbert, J. McKelvey in Advances in Molecular Modeling, Vol. 2 (Ed.: D. Liotta), JAI Press, London, 1990, pp. 65–92.
- [19] PCMODEL V 8.5, Molecular Modeling Software for Windows Operating System, Apple Macintosh OS, Linux and Unix, Serena Software, Bloomington, IN 47402–3076, USA, August 2003.
- [20] Gaussian O, Revision E.O.1, M. J. Frisch, G. W. Trucks, H. B. Schlegel, G. E. Scuseria, M. A. Robb, J. R. Cheeseman, G. Scalmani, V. Barone, B. Mennucci, G. A. Petersson, H. Nakatsuji, M. Caricato, X. Li, H. P. Hratchian, A. F. Izmaylov, J. Bloino, G. Zheng, J. L. Sonnenberg, M. Hada, M. Ehara, K. Toyota, R. Fukuda, J. Hasegawa, M. Ishida, T. Nakajima, Y. Honda, O. Kitao, H. Nakai, T. Vreven, J. A. Montgomery, Jr., J. E. Peralta, F. Ogliaro, M. Bearpark, J. J. Heyd, E. Brothers, K. N. Kudin, V. N. Staroverov, T. Keith, R. Kobayashi, J. Normand, K. Raghavachari, A. Rendell, J. C. Burant, S. S. Iyengar, J. Tomasi, M. Cossi, N. Rega, J. M. Millam, M. Klene, J. E. Knox, J. B. Cross, V. Bakken, C. Adamo, J. Jaramillo, R. Gomperts, R. E. Stratmann, O. Yazyev, A. J. Austin, R. Cammi, C. Pomelli, J. W. Ochterski, R. L. Martin, K. Morokuma, V. G. Zakrzewski, G. A. Voth, P. Salvador, J. J. Dannenberg, S. Dapprich, A. D. Daniels, O. Farkas, J. B. Foresman, J. V. Ortiz, J. Cioslowski, D. J. Fox, Gaussian, Inc., Wallingford, CT, 2015.
- [21] E. Toomsalu, P. Burk, J. Mol. Model. 2015, 21, 244.
- [22] a) J. N. Woodford, G. S. Harbison, J. Chem. Theory Comput. 2006, 2, 1464–1475; b) W.-H. Mu, G. A. Chass, D.-C. Fang, Int. J. Quantum Chem. 2008, 108, 1422–1434; c) R. B. Nazarski, B. Pasternak, S. Leśniak, Tetrahedron 2011, 67, 6901—6916.
- [23] a) J. Gräfenstein, D. Cremer, J. Chem. Phys. 2007, 127, 164113; b) T. Kupka, M. Stachów, E. Chełmecka, K. Pasterny, M. Stobińska, L. Stobiński, J. Kaminský, J. Chem. Theory Comput. 2013, 9, 4275 4286.
- [24] a) C. Adamo, V. Barone, Chem. Phys. Lett. 1998, 298, 113–119; b) C.
 Adamo, V. Barone, J. Chem. Phys. 1999, 110, 6158–6170; c) M. Ernzerhof,
 G. E. Scuseria, J. Chem. Phys. 1999, 110, 5029–5036; d) C. Adamo, G. E.
 Scuseria, V. Barone, J. Chem. Phys. 1999, 111, 2889–2899.
- [25] G. Scalmani, M. J. Frisch, J. Chem. Phys. 2010, 132, 114110.
- [26] a) J. Tomasi, B. Mennucci, E. Cancès, J. Mol. Struct.: THEOCHEM 1999, 464, 211–226; b) B. Mennucci, R. Cammi, J. Tomasi, J. Chem. Phys. 1999, 110, 6858–6870; c) J. Tomasi, B. Mennucci, R. Cammi, Chem. Rev. 2005, 105, 2999–3094.
- [27] A. K. Rappé, C. J. Casewit, K. S. Colwell, W. A. Goddard III, W. M. Skiff, J. Am. Chem. Soc. 1992, 114, 10024–10035.
- [28] J.-Y. Tao, W.-H. Mu, G. A. Chass, T.-H. Tang, D.-C. Fang, *Int. J. Quantum Chem.* **2013**, *113*, 975–984.
- [29] R. B. Nazarski, K. Justyna, S. Leśniak, A. Chrostowska, J. Phys. Chem. A 2016, 120, 9519–9528.
- [30] IDSCRF-RADII, D.-C. Fang, Beijing Normal University, Beijing, China.
- [31] Chemcraft, Version 1.8 (build 506); https://www.chemcraftprog.com (accessed April 12, 2017).
- [32] S. G. Smith, J. M. Goodman, J. Am. Chem. Soc. 2010, 132, 12946 12959.
- [33] a) EMSL Basis Set Library. Basis Set Exchange: v1.2.2; https://bse.pnl.gov/bse/portal (accessed Nov 18, 2016); b) D. Feller, J. Comput. Chem. 1996, 17, 1571–1586; c) K. L. Schuchardt, B. T. Didier, T. Elsethagen, L.

- Sun, V. Gurumoorthi, J. Chase, J. Li, T.L. Windus, *J. Chem. Inf. Model.* **2007**, *47*, 1045 1052.
- [34] a) R. H. Contreras, J. E. Peralta, C. G. Giribet, M. C. R. de Azua, J. C. Facelli, Annu. Rep. NMR Spectrosc. 2000, 41, 55–184; b) T. A. Ruden, O. B. Lutnæs, T. Helgaker, K. Ruud, J. Chem. Phys. 2003, 118, 9572–9581; c) T. A. Ruden, T. Helgaker, M. Jaszuński, Chem. Phys. 2004, 296, 53–62; d) O. B. Lutnæs, T. A. Ruden, T. Helgaker, Magn. Reson. Chem. 2004, 42, S117–S127; e) C. L. Dickson, C. D. Blundell, C. P. Butts, A. Felton, A. Jeffreys, Z. Takacs, Analyst 2017, 142, 621–633.
- [35] J. P. Perdew, Phys. Rev. B 1986, 33, 8822-8824; Erratum: Phys. Rev. B 1986, 34, 7406.
- [36] a) J. P. Perdew, Y. Wang, *Phys Rev. B* **1986**, *33*, 8800–8802; Erratum: *Phys. Rev. B* **1989**, *40*, 3399; b) J. P. Perdew, Y. Wang, *Phys Rev. B* **1992**, *45*, 13244–13249; c) J. P. Perdew, J. A. Chevary, S. H. Vosko, K. A. Jackson, M. R. Pederson, D. J. Singh, C. Fiolhais, *Phys. Rev. B* **1992**, *46*, 6671–6687; Erratum: *Phys. Rev. B* **1993**, *48*, 4978.
- [37] J. P. Perdew, K. Burke, M. Ernzerhof, Phys. Rev. Lett. 1996, 77, 3865 3868; Erratum: Phys. Rev. Lett. 1997, 78, 1396.
- [38] C. Adamo, V. Barone, Chem. Phys. Lett. 1997, 274, 242-250.
- [39] C. Adamo, V. Barone, J. Chem. Phys. 1998, 108, 664-675.
- [40] a) W.-M. Hoe, A. J. Cohen, N. C. Handy, Chem. Phys. Lett. 2001, 341, 319–328; b) N. C. Handy, A. J. Cohen, Mol. Phys. 2001, 99, 403–412.
- [41] A. J. Cohen, N. C. Handy, Mol. Phys. 2001, 99, 607-615.
- [42] P. J. Wilson, T. J. Bradley, D. J. Tozer, J. Chem. Phys. 2001, 115, 9233-9242
- [43] T. Yanai, D. P. Tew, N. C. Handy, Chem. Phys. Lett. 2004, 393, 51 57.
- [44] O. A. Vydrov, G. E. Scuseria, J. Chem. Phys. 2006, 125, 234109.
- [45] A. D. Boese, J. M. L. Martin, J. Chem. Phys. 2004, 121, 3405-3416.
- [46] a) J. Heyd, G. E. Scuseria, J. Chem. Phys. 2004, 121, 1187–1192; b) A. F. Izmaylov, G. Scuseria, M. J. Frisch, J. Chem. Phys. 2006, 125, 104103; c) A. V. Krukau, O. A. Vydrov, A. F. Izmaylov, G. E. Scuseria, J. Chem. Phys. 2006, 125, 224106; d) T. M. Henderson, A. F. Izmaylov, G. Scalmani, G. E. Scuseria, J. Chem. Phys. 2009, 131, 044108.
- [47] Y. Zhao, D. G. Truhlar, J. Chem. Phys. 2006, 125, 194101.
- [48] Y. Zhao, D. G. Truhlar, Theor. Chem. Acc. 2008, 120, 215-241; Erratum: Theor. Chem. Acc. 2008, 119, 525.
- [49] J.-D. Chai, M. Head-Gordon, J. Chem. Phys. 2008, 128, 084106.
- [50] J.-D. Chai, M. Head-Gordon, Phys. Chem. Chem. Phys. 2008, 10, 6615–6620.
- [51] A. Austin, G. Petersson, M. J. Frisch, F. J. Dobek, G. Scalmani, K. Throssell, J. Chem. Theory Comput. 2012, 8, 4989–5007.
- [52] T. Chai, R. R. Draxler, Geosci. Model Dev. 2014, 7, 1247 1250.
- [53] a) A. Bagno, F. Rastrelli, G. Saielli, J. Phys. Chem. A 2003, 107, 9964–9973; b) A. Bagno, F. Rastrelli, G. Saielli, Chem. Eur. J. 2006, 12, 5514–5525.
- [54] W. Migda, B. Rys, Magn. Reson. Chem. 2004, 42, 459-466.
- [55] S. Wolfe, B. M. Pinto, V. Varma, R. Y. N. Leung, Can. J. Chem. 1990, 68, 1051 – 1062.
- [56] a) E. Juaristi, G. Cuevas, The Anomeric Effect, CRC, Boca Raton, FL, 1994; b) I. V. Alabugin, K. M. Gilmore, P. W. Peterson, WIREs Comput. Mol. Sci. 2011. 1, 109–141.
- [57] R. Riccio, G. Bifulco, P. Cimino, C. Bassarello, L. Gomez-Paloma, Pure Appl. Chem. 2003, 75, 295–308.
- [58] a) C. D. Grimmer, C. A. Slabber, Magn. Reson. Chem. 2015, 53, 590—595;
 b) S. Hackbusch, A. Watson, A. H. Franz, Arkivoc 2017, part v, 268–292.
- [59] "Jacob's Ladder of Density Functional Approximations for the Exchange-Correlation Energy": J. P. Perdew, K. Schmidt in *Density Functional Theory and its Application to Materials* (Eds.: V. Van Doren, C. Van Alsenoy, P. Geerlings), American Institute of Physics, Melville, NY, 2001; AIP Conf. Proc. 2001, 577, 1–20.
- [60] T. Bally, P. R. Rablen, J. Org. Chem. 2011, 76, 4818-4830.
- [61] M. W. Lodewyk, M. R. Siebert, D. J. Tantillo, Chem. Rev. 2012, 112, 1839– 1862.
- [62] E. Torres, G. A. A. DiLabio, J. Phys. Chem. Lett. 2012, 3, 1738-1744.
- [63] a) "The Electron Density as Calculated From Density Functional Theory":
 R. J. Boyd, J. Wang, L. A. Eriksson in Recent Advances in Density Functional Methods, Part I (Ed.: D. P. Chong), World Scientific, Singapore, 1995, Chap. 10, pp. 369–401; b) J. Wang, L. A. Eriksson, B. G. Johnson, R. J. Boyd, J. Phys. Chem. 1996, 100, 5274–5280; c) J. Wang, B. G. Johnson, R. J. Boyd, L. A. Eriksson, J. Phys. Chem. 1996, 100, 6317–6324.

11





- [64] a) J. C. Slater, Phys. Rev. 1951, 81, 385-390; b) J. C. Slater, Quantum Theory of Molecules and Solids. Vol. 4: The Self-Consistent Field for Molecules and Solids, McGraw-Hill, New York, 1974.
- [65] A. D. Bochevarov, R. A. Friesner, J. Chem. Phys. 2008, 128, 034102.
- [66] M. G. Medvedev, I. S. Bushmarinov, J. Sun, J. P. Perdew, K. A. Lyssenko, Science 2017, 355, 49–52.
- [67] T. Gould, J. Chem. Theory Comput. 2017, 13, 2373-2377.

[68] P. D. Mezei, G. I. Csonka, M. Kállay, J. Chem. Theory Comput. 2017, 13, 4753–4764.

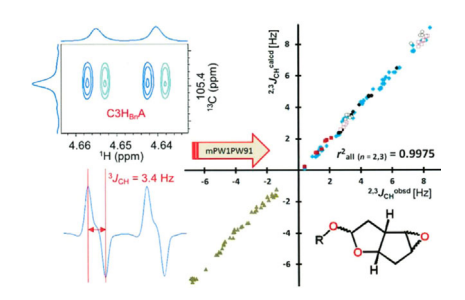
Manuscript received: October 16, 2017

Revised manuscript received: November 17, 2017 Accepted manuscript online: November 23, 2017

Version of record online: ■■ ■ , 0000

ARTICLES

Accuracy assessment: Reliable prediction of NMR parameters is crucial for conformation analysis of (bio)organic systems. The accuracy of 53 DFT methods (embracing 27 functionals and up to nine NMR-specialized basis sets) in calculations of coupling constants is benchmarked against 225 experimental $^nJ_{CH}$ (n=1–3) values of six diastereomeric tricyclic epoxides in CDCl₃ solution (see figure).



J. Adamson, R. B. Nazarski,* J. Jarvet, T. Pehk, R. Aav

Shortfall of B3LYP in Reproducing NMR $J_{\rm CH}$ Couplings in Some Isomeric Epoxy Structures with Strong Stereoelectronic Effects: A Benchmark Study on DFT Functionals

13

www.chemphyschem.org